Medbiotech Journal

MBTJ, 1(1): 001-008, 2017

Research Paper

A new attempt to introduce efficient inhibitors for Caspas-9 according to structure-based Pharmacophore Screening strategy and Molecular Dynamics Simulations

Seyed Mojtaba Mostafavi *[,a], Kowsar Bagherzadeh [b], Masoud Amanlou [b]

[a] Department of Chemistry, K. N. Toosi University of Technology, Tehran, Iran

[b] Department of Medicinal Chemistry, Faculty of Pharmacy and Pharmaceutical Sciences Research Center, Medical Sciences, University of Tehran 14155-6451, Iran

Received: 21 December 2016 Accepted: 03 February 2017 Published: 01 March 2017

Abstract

Caspases are enzymes which are the main pathway for apoptosis. Any irregulation in their functions causes increase or decrease cell death which result in autoimmune or cancer respectively. Structure-based pharmacophore drug discovery method was used to discover selective inhibitors for Caspase-9 as the initiator Caspase through effective pathway in Alzheimer's disease, through virtual screening. A pharmacophore model was developed by investigating essential interactions between the reported potent inhibitors employing a docking analysis methodology. After pharmacophore virtual screening, 9 compounds from both National Cancer Institute (NCI) and ZINC databases were filtered as potent inhibitors of Caspase-9. The efficiency of the discovered compounds was further monitored by docking studies.

Keywords: Alzheimer's disease; Virtual screening; Pharmacophore; Docking, Caspase-9; Inhibitor

How to cite the article:

S. M. Mostafavi, K. Bagherzadeh, M. Amanlou A new attempt to introduce efficient inhibitors for Caspas-9 according to structure-based Pharmacophore Screening strategy and Molecular Dynamics Simulations Medbiotech J. 2017; 1(1): 001-008, DOI: 10.22034/MBT.2017.60325

1. Introduction

Apoptosis is a programmed cell death which is a crucial process in development, the maintenance of cell homeostasis and regulation of immune system. When the apoptosis is either excessive or insufficient, it can play an effective role in many disease including cancer, autoimmune disease, viral infection and neurological disorders [1,2].

In mammalian, apoptosis is activated throughout three main pathways by caspase enzymes which their names extracts from their ability in cleavage of substrates after an Asp residue [3]: the extrinsic, (death receptor pathway), the intrinsic (apoptosome pathway) and the cytotoxic lymphocyte-initiated granzyme B pathway [4]. In extrinsic and intrinsic pathways, apoptosis is driven by Caspases from initiators (caspase-8,9) to effectors (caspase-3,7). Thus, activation and inhibition of initiator Caspases contains a central regulatory step in cellular physiology [5] and has made Caspases considerable targets to design cytoprotective drugs. Also, the inhibition of excessive apoptosis disease is considered as the main ways to treat or reduce signs of disease [6-12]. Oxidative damage, by aging and disease, leads to mitochondria dysfunction, releasing cytochrome C and then activates Caspase-9 that is continued by effectors Caspases [13]. There are some evidences which cleavage of Asp421 by Caspases is more rapid in tau cleavage, so Capases activation can hyperphosphorilize tau proteins and they have effective rules in Amyloid precursor protein (APP) and tau cleavages [14,15]. Enhancement in tau

proteins increases neurofibrillary tangles (NFTs) [13].
Extracellular plaques of amyloid-β and intercellular neurofibrillary tangles (NFTs) are defined in Alzheilmer's disease as a progressive disorder [16]. Since Caspase-cascade is a very effective pathway for apoptosis [17,18], here in Caspase-9 inhibition has been studie Caspase-9 inhibition is studied at this paper. Caspase-9 belongs to initiator class of Caspases, which is activated by death stimulus in upstream, so its inhibition role causes stopping the death cell during the caspase cascade [17,19,20].
Caspases have a special recognition sequence including at least four N-terminal amino acids in their active site [1,21]. Active site in caspase-9 is recognized by a four -aminoacid sequence (LEHD) involving an aspartic acid residue in the P1 position and a small hydrophobic residue in the P2 position , in CARD domain from caspase-3, 7 then by limited proteolysis change them to active forms [1, 21-24].
Structure-based pharmacophore model generating from the optimal interactions of already experimentally reported inhibitors with the target macromolecular is defined as a very helpful method for screening a ligand database to fine the more coinciding to the model so more effective inhibitors. Then, the obtained information enable medicinal chemists to develop molecules with higher binding affinities for the target macromolecule and can be used to generate specific biological responses [23].
In this study, a computational design of small molecular inhibitors for Caspase-9 is done by developing and modifying a pharmacophore model based on teripeptidyl inhibitor (PHQ-GLU-VAL-ASP) which is recrystallized in the Protein Data Bank file (pdb code 1jxq) by employing docking strategy.

2. Materials and methods

2.1 Enzyme structure preparation

Enzyme Caspase-9 structure file was obtained from RCSB Protein Data Bank (pdb code, 1 jxq, 2.80 Å) [18,19]. The pdb structure was refined due to a large missing part in the crystallographic structure. This missing sequence contained 35 amino acids (ASTSPEDESPGSNPEPDATPFQEGLRTFDELDAIS).
Homology modeling strategy is applied to fix the large gap in the structure. Since no crystallographic structure with an acceptable similarity to that of caspase-9 with no missing by complete amino acid sequencing, Caspase-9 structure was found by blasting the enzyme sequence employing the online program BLAST from NCBI, it was decided to solely homology model the missing part. The target sequence is aligned to those with similar sequence to identify appropriate templates for the subsequent homology modeling procedure. MODELER 9.10 [25] employed four structures with PDB IDs of 4DGE, 4DGA, 2PBj, and 1Z9H as the appropriate templates to build the missed part structure of Caspase-9. While the obtained structure mainly contains loops and turns, a α-helics (DELDAIS) and a β-sheet (ASTS) are also observed. This structure was linked to that of the crystallographic one with the aid of Hyperchem 8.0 and then, GROMACS MD package 4.5.5 and GROWMOS96 53ab as classical molecular dynamic simulations (MDs) is used for minimizing and optimizing of energy and an appropriate structure was achieved after 40 nanoseconds of MDs (Figure 1). The ramachandran plot of the enzyme average structure during the equilibration state was plotted and is shown in Figure 2. As it is obvious, only 4 amino acids of the modeled sequence are in the forbidden region and two out of four are Gly that can be present in both regions. Therefore, the obtained overall enzyme was employed for the rest of the study.

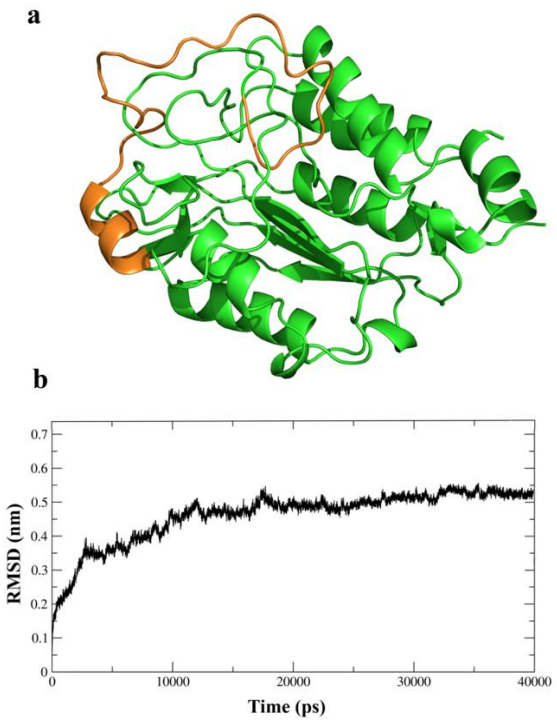

Figure 1. a) The protein structure after classical molecular dynamic simulations, the target sequence is shown in orange color, b) The backbone root mean square deviations (RMSD) plot of the enzyme during 40 nanoseconds of simulations.

2.2 Validation of Autodock accuracy and performance

For validation of docking method in the best docked conformation, RMSD (root mean square deviation) is <2.0 Å that is extracted from experimental and the used scoring function is acceptable [26]. In our validation, RMSD values were excellent for the native ligand, which was 0.623 Å.
2.3 Docking methodology

Autodock tools 1.5.4 was used for preparing input files. The grid maps were calculated and the docking procedure was performed by Auto grid 4.2 and Auto dock 4.2, respectively. Ligands docked on Caspase-9 were those from binding database, reported up to August 2012 [27].

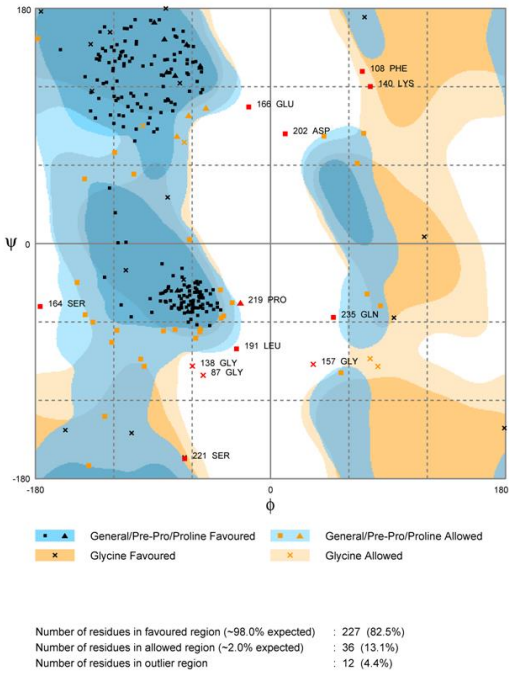

Figure 2. The Ramachandran plot of the enzyme average structure during the equilibration state, the filled red color points represent the target sequence residues.

The grid box of 126, 126, 126 Å (x, y and z) as the large grid box and 66, 66, 68 Å (x, y and z) as the small grid box were assigned on caspase-9 binding pocket with the spacing of 0.375 Å. Other docking study parameters were as follow: number of Lamarckian job = 100; initial population =100; maximum number of energy evaluation =25×105; maximum generations =27000; mutation rate of 0.02.; a crossover rate of 0.80.

2.4 Pharmacophore model generation and virtual screening

Structure based pharmacophore model approach was used for considering the ligands modes of interactions in the protein binding pocket. Ligandscout v.301 software was employed for development and refinement of all pharmacophore models [28]. The obtained models were then used as filters during virtual screening by Ligandscout v.301 to extract ligands with desired pharmacophore features from NCI and ZINC compound databases (each compound in its 25 conformers).

2.5 Classical molecular dynamic simulations

GROMACS MD package 4.5.5 and GROWMOS96 53ab force field are reinforced for classical molecular dynamic simulations [29]. PRODRG server was applied to obtain the ligand's topology files [30]. The initial structure that contained Caspase-9 in complex with the target ligand in their best mode of interaction according to the calculated binding energy and orientations in the binding pocket was derived from the former docking studies. The desired complex was immerged in a dodecahedron-shaped box (X, Y and Z) with minimum distance of 1nm from each edge of the box, while, periodic boundary conditions were also assigned in all directions. Some Na+ counter ions were substituted by water molecules randomly to neutralize the system net charge. Steepest descent algorithm was employed to minimize energy of system. The system went through NVT ensemble MD simulations for 20ps right after convergence followed by simulations under NPT ensemble at 300 K. Berendsen barostat and thermostat were used to keep the pressure and temperature constant at 1 bar and 300 K with a coupling time of tp=.5ps, tt=.1ps, respectively. The partial mesh Ewald method was used to calculate long-rage electrostatic interactions. For restraining, the bond lengths LINCS was employed with an integration step of 1 fs. The MD simulations were extended NPT for 10 nanoseconds at constant pressure and temperature conditions.

2.6 Data analysis and presentation software

LigandScout v3.01, Autodock tools 1.5.4, Discovery studio v3.5 and PyMOL software were used to analyze and visualize all ligand–protein interactions. PyMOL was also employed to better illustrate ligand-proteins modes of interactions for MD simulations studies.

3. Results

A Structure-based pharmacophore model was generated according to a three amino acid peptide in the crystallised structure of the caspase-9 protein. The model was further modified according to the structure of the active pocket. These structure-based generated models (models 2-pharmacophore) virtual screening resulted in 19 compounds to be considered as caspase-9 inhibitors. To specify more, docking by a small grid box on active site was done on 19 compounds in model 2-pharmacophore which finally 9 compounds was achieved. The extracted compounds affinities were ranked by employing docking methodology. Rigid docking studies were carried out using Autodock 4.2, and the results are presented in Table1. Pharmacophore virtual screening is took out on out some compounds according to their similarity to the models and then are followed by docking

methodology to extract the ones with higher affinity for the active site. According to the docking studies results, models 2-pharmacophore resulted in 9 compound with considerable affinities for the active site. The proper compounds were chosen based on their docking binding energy value, drug like parameters and also their orientation in the pocket. Further bioassay studies are highly recommended to be performed on the obtained compounds. Among obtained compounds, 2a was selected as the best because of the best binding energy, including critical interaction by Amino acids in active site of pocket of receptor. Molecular dynamics was carried out on 2a as the best parameters to interact with caspase-9.

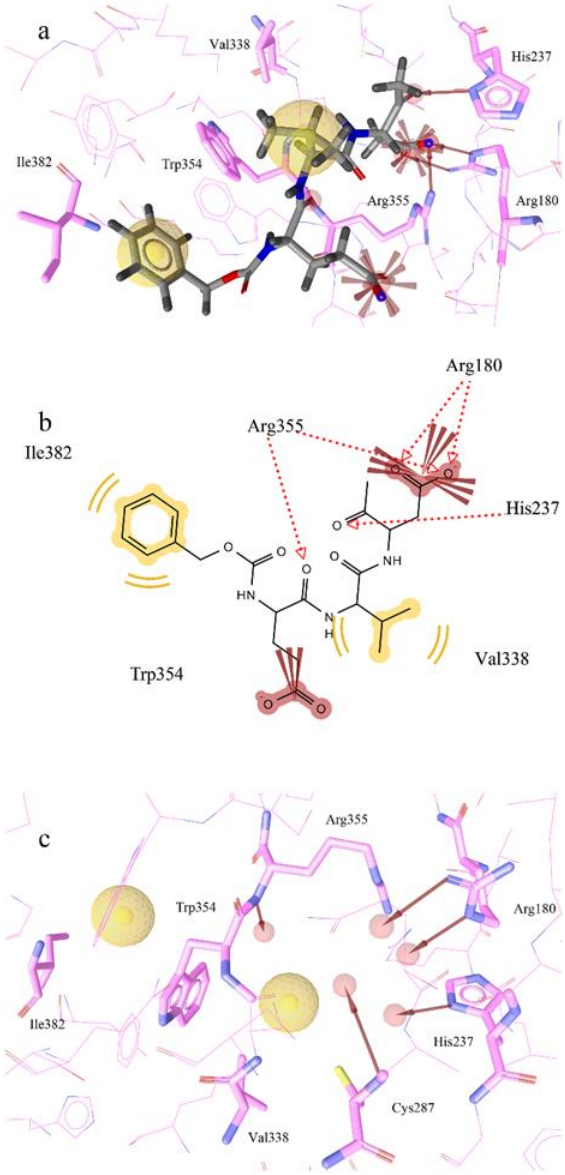

Figure 3. a) Pharmacophore model (model 1)generated from 1JXQ/tripeptidyl sequence PHQ-GLU-VAL-ASP a. red arrows; HBA, yellow spheres; hydrophobic sites, gray spheres; excluded volumes, and red stars; negative ionizable interactions. b. the pharmacophore model interactions with the active pocket residues. c. The modified pharmacophore model (model 2-pharmacophore), (red arrows; HBA, yellow spheres; hydrophobic sites, gray spheres; excluded volumes).

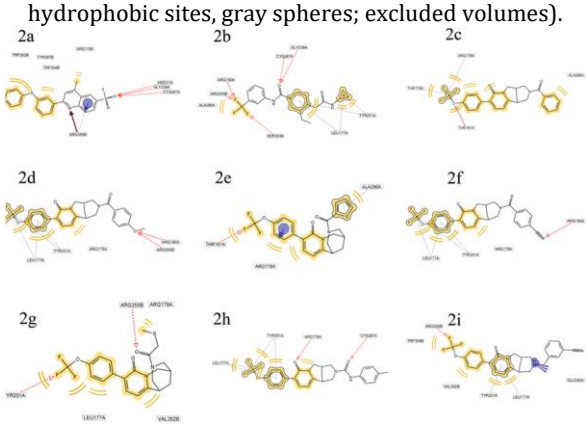

Figure 4. The compounds elicited from pharmacophore screening of model 1-pharmacophore (Figure 1-c) after docking studies

4. Disscusion

Protein crystallography structure is included two-chain caspase 9 which missed first 138 residue by proteolytic removal of the CARD. The crystal contains teripeptidyl inhibitor in active site [22]. It should also be mentioned that Arg 355, Arg 180, His 237, Cys 287 are the key amino acids of the active pocket of enzyme caspase-9 as it was already reported in the literature [22, 23, and 31]. Further, hydrophobic and H-bonding interactions are the main contacts between the ligands and the active site. The crystallographic structure and the peptide sequence in the active site were studied thoroughly and were used for pharmacophore model generation. Model1-pharmacophore was generated focusing on the interactions of a teripeptidyl sequence PHQ-GLU-VAL-ASP trapped in the active pocket (Figure 3.a). The model 1 includes H-bond acceptors (red arrows) which shows that there are 4 H-bond acceptors via His237, Arg180 and and Arg355 [22, 23, 31]. Further, a hydrophobic area has been created in Ile382, Trp354 and Val338 area. The two negative ionizable interactions occur as a result of the carboxylate functional groups of the peptide amino acids (Glu and Asp).

By virtual screening of the database of the pharmacophore model1-pharmacophore, no Coincident structure with this model was obtained. Consequently, to broaden the applicability of the model, the number of pharmacophores was reduced by omitting the two negative ionizable pharmacophores .To more specify Model 2-pharmacophore, the techniques of structure-based pharmacophore modeling was used and a hydrogen bond acceptor pharmacophor with original position (Orig. Pos.) 23.80, 43.67 and -8.98, tolerance 1.5, and weight 1, was created through NH functional

group of Cys287 (model 2-pharmacophore, Figure 3.c).

Model 2-pharmacophore screening resulted in 19 compounds, which after docking studies by a blind dock on active pocket, 9 compounds (2a-i, Figure 4) were found to have better affinities and orientation to interact with the critical residues of the Caspase-9 active site. The exact type of these compounds interactions and binding energies were further investigated. Docking procedure was repeated assigning small grid box on the active site, and the final results are reported in Table 1.

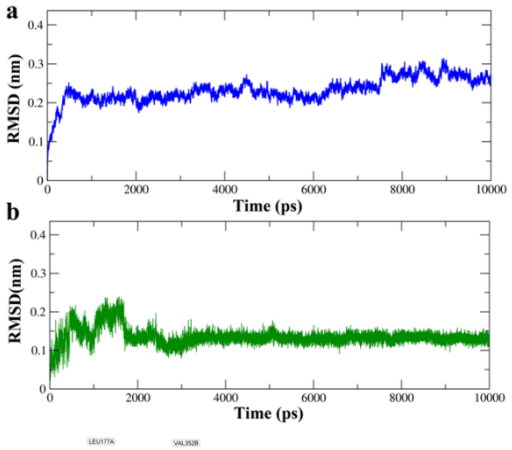

Figure 5. RMSD plots of a) Caspase-9 backbone in complex with ligand 2a (blue), and b) Ligand 2a backbone in complex with caspase-9, during 10 nanoseconds of MD simulations

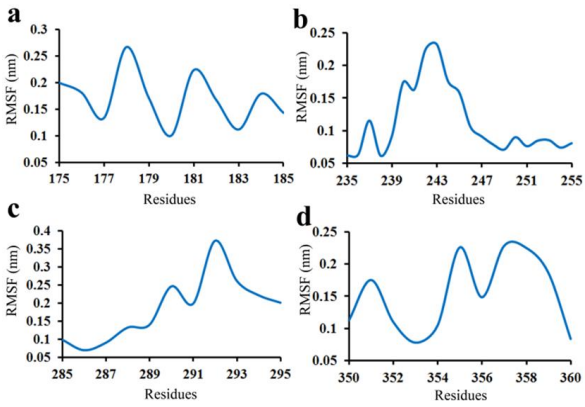

Figure 6. RMSF plots of caspase-9 residues in complex with ligands 2a, **a**) residues 175-185, **b**) residues 235-255, **c**) residues 285-395, **d**) residues 350-360.

4.1 Molecular Dynamic Simulations

According to the calculated docking binding energy value and its modes of interactions, an appropriate conformation of the most potent ligand in complex with caspase-9 that is obtained to be compound 2a. The complex of Compound 2a with Caspase-9 was assigned to classical molecular dynamic simulations to further evaluate the obtained binding pose stability and the ligands consistency in the active pockets in a dynamic environment while the solvent effects are also included. The backbone root mean square deviations (RMSD) of the protein backbone as well as the ligand itself were plotted with respect to their initial structure (the energy minimized structure) and as a function of the simulation time to ensure the system reached the equilibration state. As it can be seen in Figure 5, no significant deviations are observed for both the protein backbone and the ligand which indicates the efficiency of the established interactions Between them. As matter, while notable deviations are observed in the ligand conformation for the establishment of efficient interactions in caspase-9 binding pocket in the first 3 nanoseconds of the simulation time which then almost becomes fix in its position, the protein does not need to go under significant conformational changes for the formation of a conducive binding.

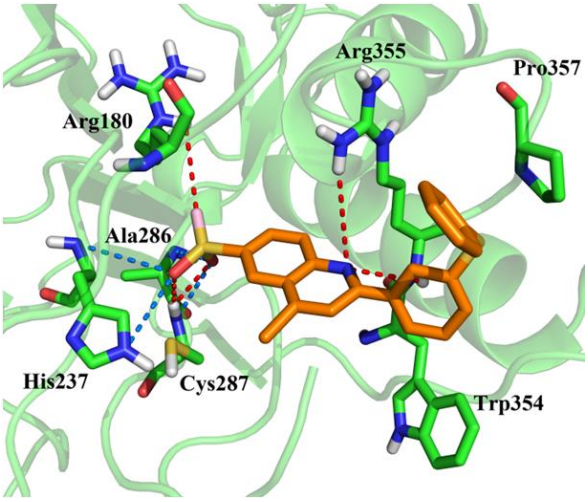

Figure 7. The studied ligands average positions in the active pocket, the red dashes represent hydrogen bonds and the blue dashes represent salt bridges

Further, to better observe the enzyme residues behavior throughout MD simulations time, root mean square fluctuations (RMSF) of the amino acids were calculated and graphed. According to Figure 4, residues Arg180, His237, Gly238, Tyr251, Ala286, Cys287, Trp354 show the least fluctuations while because of their presence in pliable parts of the protein, loop and turn structures. This rigidity can be attributed to the involvement of the mentioned residues in interaction with the ligand. Also a very significant fluctuation is observed for residue Pro357 (Figure 6) shows that this residue needs to change its orientations in order to establish better electrostatic interactions with the diphenyl sulfide fragment of the compound.

According to the results came at hand via performed molecular dynamic simulations, the

compound stay firm in the binding pose obtained from the docking studies and is stabilized in the pocket by the interactions discussed. The studied ligand average position during 10 nanoseconds of MD simulations is shown in Figure 7 Several hydrogen bonds are formed between compound 2a and Arg180, Cys287, Arg355 and Trp354 (the red dashes). Also electrostatic interactions presence between diphenyl sulfide benzene rings and residues Trp354 and Pro357 are quite inevitable. Also, the fluorphosphate fragment enables several salt bridge formations as well.

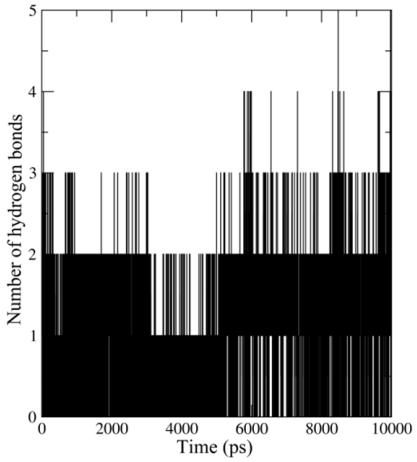

Figure 8 . Number of hydrogen bonds evolvement during 10 nanseconds of simulations time

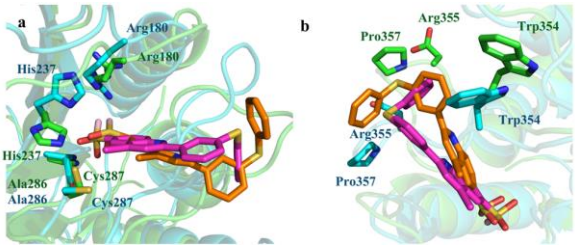

Figure 9. The superimposed structures of the energy minimized ligand-protein complex (ligand is shown in magneta and the protein in cyan) the one after 10 nanoseconds of MD simulations (ligand is shown in orange and the protein in green). To avoid complications, **a**) represents interactions of diphenyl sulfide fragment, and **b**) represents quinoline and fluorphosphate fragments.

The stability of the hydrogen bonds formed between the ligand and active pocket residues was computed as well. Based on Figure 8, as the simulations progress, the hydrogen bonds number increases as well, which shows that the dynamic nature of the simulations method give the chance to both protein and the ligand to fit into their best conformations where they can conduct productive interactions. Further, this phenomenon provide more evidences the ligand stability in caspase-9 binding pocket.

The catalytic site structures of caspase-9 enzyme after energy minimization and 10 nanoseconds of MD simulations were superimposed to get a better insight of the impact of the dynamic environment of the modes of interactions. As it is presented in Figure 9, the residues (Trp354, Pro357 and Arg355) orientations that are interacting with diphenyl sulfide fragment has changed dramatically as well as the conformation of the target fragment itself, but the mode of interactions (π-π electrostatic interactions) has not changed. In contrast, quinoline as well as fluorphosphate fragments seems to have stayed almost fixed in their positions which is due to the establishment of hydrogen bonds, salt bridges and also protonated salt bridges with keeps both ligand and the residues involved firm as well as the rigid nature of this part of the ligands structure.

Acknowledgment:
This study was supported by a grant from the Research Council of Tehran University of Medical Sciences.

References

1.Thomas Rudel (1999) Caspase Inhibitors in Prevention of Apoptosis. Herz . 24, 236-41.
2. Robert V. Talanian, Kenneth D. Brady, Vincent L. Cryns (2000) Caspases as Targets for Anti-Inflammatory and Anti-Apoptotic Drug Discovery. Journal of medicinal chemistry 43 (18), 3351-33710
3. Yigong Shi (2002) Mechanisms of Caspase Activation and Inhibition during Apoptosis. Molecular Cell 9, 459–470.
4. SP Cullen, SJ Martin (2009) Caspase activation pathways: some recent progress. Cell Death and Differentiation 16, 935-938.
5. S. Parvanian, et al.,Multifunctional nanoparticle developments in cancer diagnosis and treatment, Sensing and Bio-Sensing Research (2016), http://dx.doi.org/10.1016/j.sbsr.2016.08.002.
6. Hiroyuki Yaoita, Kazuei Ogawa, Kazuhira Maehara, Yukio Maruyama (1998) Attenuation of Ischemia/Reperfusion Injury in Rats by a Caspase Inhibitor. Circulation 97, 276 – 281.
7. J.S. Braun, R. Novak, K. H. Herzog, S.M. Bodner, J.L. C leveland, E.I. Tuomanen . (1999) Neuroprotection by a caspase inhibitor in acute bacterial meningitis. Nature Medicine. 5, 298–302.
8. Raffaele Cursio, Jean Gugenheim, Jean Ehrland Ricci, Dominique Crenesse, Philippe Rostagno, Laurence Maulon, Marie-Christine Saint-Paul, Bernard Ferrua , Patrick Auberger (1999) A caspase inhibitor fully protects rats against lethal

normothermic liver ischemia by inhibition of liver apoptosis. The Journal of Federation of American Societies for Experimental Biology 13, 253 – 261.
9. S. R. Grobmyer, R. C. Armstrong, S. C. Nicholson, C. Gabay, W. P. Arend, S. H. Potter, M. Melchior, L. C. Fritz, and C. F. Nathan (1999) Peptidomimetic fluoromethylketone rescues mice from lethal endotoxic shock. Molecular Medicine 5, 585 – 594.
10. JÖrg B. Schulz, Michael Weller, Michael A. Moskowitz (1999) Caspases as Treatment Targets in Stroke and Neurodegenerative Diseases. Annals of Neurology 45, 421 – 429.
11. Dennis Lee, Scott A. Long, Jerry L. Adams, George Chan, Kalindi S. Vaidya, Terry A. Francis, Kristine Kikly, James D. Winkler, Chiu-Mei Sung, Christine Debouck, Susan Richardson, Mark A. Levy, Walter E. DeWolf Jr., Paul M. Keller, Thaddeus Tomaszek, Martha S. Head, M. Dominic Ryan, R. Curtis Haltiwanger, Po-Huang Liang, Cheryl A. Janson, Patrick J. McDevitt, Kyung Johanson, Nestor O. Concha, Winnie ChantOj, Sherin S. Abdel-Meguid, Alison M. Badger, Michael W. Lark, Daniel P. NadeautOk, Larry J. Suva, Maxine GowentOk, Mark E. Nuttall. (2000) Potent and Selective Nonpeptide Inhibitors of Caspases 3 and 7 Inhibit Apoptosis and Maintain Cell Functionality, The Journal of Biological Chemistry 275, 16007 – 16014.
12. M.M. Mocanu, G.F. Baxter, D.M. Yellon (2000) Caspase inhibition and limitation of myocardial infarct size: protection against lethal reperfusion injury, British Journal of Pharmacology 130, 197 – 200.
13. Rohn Troy T, Rissman RA, Davis MC, Kim YE, Cotman CW, Head E.(2002) Caspase-9 activation and caspase cleavage of tau in the Alzheimer's disease brain. Neurobiology Disease. 11, 341-54.
14. Tryo T. Rohn (2010) The role of caspases in Alzheimer's disease; potential novel therapeutic opportunities. Apoptosis. 15, 1403-9.
15. Troy T. Rohn, Elizabeth Head (2009). Caspases as Therapeutic Targets in Alzheimer's Disease: Is It Time to "Cut" to the Chase?. International Journal of Clinical and Experimental Pathology . 2, 108–118.
16. Zhao Zhong Chong, Faqi Li, and Kenneth Maiese (2005). Employing New Cellular Therapeutic Targets for Alzheimer's Disease: A Change for the Better?. Current Neurovascular Research 2, 55–72.
17. Jean-Bernard Denault and Guy S. Salvesen (2002) Caspases: Keys in the Ignition of Cell Death , Chem Rev 102, 4489-5500.
18. Eric N. Shiozaki, Jijie Chai, Daniel J. Rigotti, Stefan J. Riedl, Pingwei Li, Srinivasa M. Srinivasula, Emad S. Alnemri, Robert Fairman (2003) Mechanism of XIAP-mediated inibition of caspase-9. Molecular Cell 11, 519–527.
19. A. Philchenkov (2004) Caspases: potential targets for regulating cell death. Journal of Cellular and Molecular Medicine 8, 432-444.
20. GM Cohen (1997) Caspases: The executioners of apoptosis. Biochem Journal. 326, 1-16.
21. Markus G Grütter (2000) Caspases: key players in programmed cell death. Current Opinion in Structural Biology, 10,6, 649-655.
22. Martin Renatus, Henning R. Stennicke, Fiona L. Scott, Robert C. Liddington, and Guy S. Salvesen (2001) Dimer formation drives the activation of the cell death protease caspase 9, Proceedings of the National Academy of Sciences (PNAS) 98 , 14250–14255.
23. Atsushi Yoshimori, Junichi Sakai, Satoshi Sunaga, Takanabou Kobayashi, Satoshi Takkahashi, Naoyuki Okita, Pyoko Takasawa, Sei-ichi Tanuma (2007) Structural and functional definition of the specificity of a novel caspase-3 inhibitor, Ac-DNLD-CHO, BMC pharmacology, 7, 1471-2210.
24. Wu Yang, John Guastella, Jin-Cheng Huang, Yan Wang, Li Zhang, Dong Xue, Minhtam Tran, Richard Woodward, Shailaja Kasibhatla, Ben Tseng, John Drewe and Sui Xiong Cai (2003) MX1013, a dipeptide caspase inhibitor with potent in vivo antiapoptotic activity, British Journal of Pharmacology 140, 402–412.
25. A. Šali and T. L. Blundell (1993) Comparative protein modelling by satisfaction of spatial restraints. Journal of Molecular Biology 234, 779-815.
26. Renxiao Wang , Yipin Lu , Shaomeng Wang (2003). Comparative evaluation of 11 scoring functions for molecular docking. Journal of Medicinal Chemistry, 46, 2287-2303.
27. Liu, T., Lin, Y., Wen, X., Jorissen, R. N., & Gilson, M. K. (2007). BindingDB: A web-accessible database of experimentally determined protein–ligand binding affinities. Nucleic Acids Research 35, D198–201.
28. G.Wolber, T.Langer (2005) LigandScout: 3-D pharmacophores derived from protein-bound ligands and their use as virtual screening filters. Journal of Chemical Information and Modeling 45, 160-169.
29. Pronk, S., Pall, S., Schulz, R., Larsson, P., Bjelkmar, P., Apostolov, R., Lindahl, E. (2013). GROMACS 4.5: A high-throughput and highly parallel open source molecular simulation toolkit. Bioinformatics 29, 845–854.
30. Schuttelkopf, A. W., & van Aalten, D. M. (2004). PRODRG: A tool for high-throughput crystallography of protein–ligand complexes. Acta crystallographica Section D: Biological Crystallography 60, 1355–1363.
31. Yang chao, Eric N. Shiozaki, Srinivasa M. Srinivasula, Daniel J. Rigotti, Robert Fairman, Yigong Shi (2005) Engineering a Dimeric Caspase-9: A Re-evaluation of the Induced Proximity Model for Caspase Activation, PloS Biology 3,1079-1087.

Table1. Details of the best ligands elicited from pharmacophor search based on docking studies: Ligand=the given name of the compound; LS pharmacophore features = number of LigandScout pharmacophore features (aro = aromatic ring; hyd = hydrophobic sphere; don = H-bond donor; acc = H-bond acceptor; pos=positively charged group); H-bond contacts = residues with which ligand makes hydrogen bond contacts; xlogP= Partition coefficient , Binding energy= Binding energy from the docking studies [a] determined according on Zinc database

Ligand	Binding Energy	LS pharmacophore feature	H-bond contacts	MW	xlogP [a]
2a	-9.29	3 hyd, 2 acc, 1 aro	Arg 335, Gly 238, Cys 287	409	6.26
2b	-6.89	3 hyd, 3 acc	Arg 355, Arg 180, Cys 287, Ser 353, Gly 238	397.441	4.05
2c	-7.12	4 hyd, 2 acc, 1 aro	Thr 181	454.448	4.14
2d	-7.19	2 hyd, 1 acc	Arg355, Arg 180	484.474	4.20
2e	-7.08	3 hyd, 1 acc	Tyr 251	460.477	4.51
2f	-6.88	4 hyd, 2 acc, 1 aro	Arg 180, Tyr 251	479.458	3.90
2g	-6.30	5 hyd, 1 acc	Arg 355	438.471	3.43
2h	-6.63	3 hyd, 1 acc, 1 don	Arg 355, Glu 290	483.49	5.38
2i	-6.85	1 hyd, 1 acc, 1 pos	Tyr 251	466.483	4.71